

# Microelectronic neural bridge for signal regeneration and function rebuilding over two separate nerves\*

Shen Xiaoyan(沈晓燕)<sup>1,3</sup>, Wang Zhigong(王志功)<sup>1,†</sup>, Lü Xiaoying(吕晓迎)<sup>2</sup>,  
Xie Shushan(谢书珊)<sup>1</sup>, and Huang Zonghao(黄宗浩)<sup>1</sup>

<sup>1</sup>Institute of RF- & OE-ICs, Southeast University, Nanjing 210096, China

<sup>2</sup>Key Laboratory of Bioelectronics, Southeast University, Nanjing 210096, China

<sup>3</sup>School of Electronic Information, Nantong University, Nantong 226019, China

**Abstract:** According to the feature of neural signals, a micro-electronic neural bridge (MENB) has been designed. It consists of two electrode arrays for neural signal detection and functional electrical stimulation (FES), and a microelectronic circuit for signal amplifying, processing, and FES driving. The core of the system is realized in 0.5- $\mu\text{m}$  CMOS technology and used in animal experiments. A special experimental strategy has been designed to demonstrate the feasibility of the system. With the help of the MENB, the withdrawal reflex function of the left/right leg of one spinal toad has been rebuilt in the corresponding leg of another spinal toad. According to the coherence analysis between the source and regenerated neural signals, the controlled spinal toad's sciatic nerve signal is delayed by 0.72 ms in relation to the sciatic nerve signal of the source spinal toad and the cross-correlation function reaches a value of 0.73. This shows that the regenerated signal is correlated with the source sciatic signal significantly and the neural activities involved in reflex function have been regenerated. The experiment demonstrates that the MENB is useful in rebuilding the neural function between nerves of different bodies.

**Key words:** micro-electronic neural bridge; functional electrical stimulation; implantable device; functional rebuilding

**DOI:** 10.1088/1674-4926/32/6/065011

**EEACC:** 2570

## 1. Introduction

Recent development of micro-electronics opens up a new possibility for the application in the area of neurobiology. More and more micro-electronic devices are being used in biomedicine<sup>[1-3]</sup>. On the one hand, much research on the detection or the recording of neural signals has been done to analyze the structure and function of organisms or provide references for diagnosis. On the other hand, electronic devices used as functional electrical stimulation (FES) have already been used in many aspects of medical rehabilitation, including the rehabilitation of hearing<sup>[4,5]</sup>, vision<sup>[6-8]</sup>, sensory<sup>[9]</sup> and motor function<sup>[10]</sup>, especially after stroke or spinal cord injury. A common feature of those FES methods is that the pulse patterns are formed artificially. In this paper, we will study the micro-electronic neural bridge (MENB) by which the lost neural function of an injured nerve can be rebuilt under the control of the signal from the body itself.

The concept of the MENB was introduced in 2005<sup>[11,12]</sup>. In general, the MENB promoted by our research group includes both the signal detecting and the FES circuits. Since then, a series of MENB modules have been implemented in the form of hybrid integration and more than 20 runs of animal experiments have been carried out. It has been demonstrated that by means of one of our MENBs, the neural signal, externally evoked and spontaneously generated, can be regenerated in the

distal stump of an interrupted spinal cord of a rat or a rabbit, and relevant reactions of legs have been observed<sup>[13]</sup>.

However, the ultimate goal of our study is to develop a miniature implantable electronic system that can perform many signal channels in two directions to bridge an interrupted spinal cord and to ultimately rebuild the motor function. Therefore, we have made much effort to miniaturize the MENB.

In this paper, a new generation of MENB is developed. A core chip used for neural signal regeneration is designed in a standard 0.5- $\mu\text{m}$  CMOS technology (CSMC, Wuxi, China) and encapsulated in DIP14. A fully complete neural signal regeneration system based on the core chip is realized on a PCB and has been used in animal experiments. The experimental results show that the system can be used in neural signal regeneration.

## 2. Methods

### 2.1. System design of the MENB

To meet the needs of implantation, the MENB should have a low-noise but high-precision input stage and an output voltage driver stage with a low internal resistance or an output current driver stage with a high internal resistance.

According to the features of neural signals and implantable devices, the following aspects should be considered in the cir-

\* Project supported by the National Natural Science Foundation of China (Nos. 90307013, 90707005), the Natural Science Foundation of Jiangsu Province, China (No. BK2008032), the Special Foundation and Open Foundation of State Key Laboratory of Bioelectronics of Southeast University, and the Nantong Planning Project of Science and Technology, China (No. K2009037).

† Corresponding author. Email: zgwang@seu.edu.cn

Received 25 December 2010, revised manuscript received 22 March 2011

© 2011 Chinese Institute of Electronics

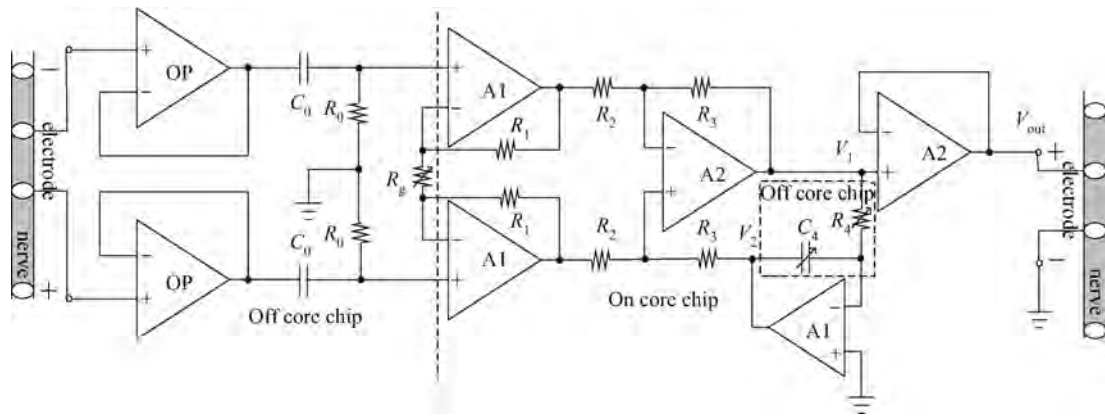


Fig. 1. Neural signal regeneration system.

circuit design<sup>[14–20]</sup>:

(1) The typical neural action potentials, or spikes, detected by a pair of electrodes near a nerve have amplitudes of up to 500  $\mu\text{V}$  when recorded extracellularly, with energy in the 100 Hz–7 kHz band.

(2) The internal resistance of the equivalent voltage source lies in the range of 5–30 k $\Omega$ .

(3) Many ECG (electrocardiogram) and EMG (electromyogram) signals may be coupled into the detecting circuit and act as interferences.

(4) The interface between an electrode and the surrounding organism could have a large DC offset, which can influence the work of the detecting circuit.

(5) The power dissipation must be low, because the organism is sensitive to temperature change.

A core chip is used in the MENB and manufactured in a standard 0.5  $\mu\text{m}$  CMOS process (CSMC, Wuxi, China) and encapsulated in DIP14. The circuit diagram of our new MENB version is shown in Fig. 1. It consists of a head stage, a filtering network, a preamplifier, an integral filter, and a voltage follower. As the basic cells of the circuit, two types of OPAs (operational amplifiers) were designed with low power, low noise, small size, high gain, and high CMRR (common-mode rejection ratio)<sup>[21]</sup>. They were used in different modes. Among them, A1 is a two-stage OPA, and A2 is a constant- $g_m$  OPA with rail-to-rail input and output voltages for low-voltage supply and full-swing driving capability.

As the first stage, the noise performance of the head stage is critical to the whole system. Therefore, it should be of low noise. Because of the high and unstable resistance of the organism, the equivalent current noise is mainly considered. Thus, a differential unit-gain buffer was used as the head stage. This is not only for their high resistance but also for their effective isolation for the next stage.

The design of the pre-amplifier circuit is also very challenging, because the neural signal detected by the electrode is very weak. Therefore, a 3-OPA instrumentation amplifier is generally used as the input stage in bioelectric measurements. High input impedance and high CMRR can be obtained without extensive trimming. Considering the possible polarization voltage, AC coupling was accepted. Since many useful biological signals include low frequency components, it is hard to choose the cutoff frequency of the filter. We have to make a

compromise between the bandwidth and the baseline drifting. If the cutoff frequency is too low, the circuit will be blocked when there is a high pulse at the input of the circuit and it will take a long time for the baseline to recover. Therefore, we have chosen an integral circuit as the feedback circuit for the 3-OPA instrumentation amplifier. The circuit consists of  $R_4$ ,  $C_4$ , and an operational amplifier. Thus, the integral circuit and the instrumentation amplifier build up the preamplifier stage with a high pass feature. The gain of the circuit can be adjusted among 550, 1340, and 2000, according to  $R_g$ 's value. The cutoff frequency can be calculated as

$$f_{\text{HP}} = \frac{1}{2\pi R_4 C_4}. \quad (1)$$

The simulated equivalent input noise is 27 nV and the simulated power dissipation is 4.11 mW.

Figure 2(a) shows the die of the neural signal regeneration system that has been realized in the 0.5  $\mu\text{m}$  CMOS process of CSMC (Wuxi, China). The area is  $0.99 \times 0.934 \text{ mm}^2$ . Figure 2(b) shows the packaged chip of DIP14 form.

Figure 2(c) shows the PCB-system of the MENB, which is used in animal experiments successfully.

The gain is

$$A_v = -\frac{R_3}{R_2} \left( 1 + \frac{2R_1}{R_g} \right). \quad (2)$$

$A_v$  can be adjusted by changing the external resistor  $R_g$ .  $R_1 = 20 \text{ k}\Omega$ ,  $R_2 = 20 \text{ k}\Omega$ , and  $R_3 = 265 \text{ k}\Omega$  were integrated on chip.

## 2.2. Experimental set-up

The MENB that we implemented has been used in a series of animal experiments. For the sake of avoiding the conduction of the organism itself, or introduction of other interference, we have designed the neural regeneration experiment on the sciatic nerves of separate spinal toads, i.e. the sciatic nerve signals of one toad were transmitted to and regenerated on the sciatic nerve of another toad by the MENB system. The experimental set-up is sketched in Fig. 3.

All experimental procedures were in accordance with the guidelines of the National Institute of Health Guide for the Care

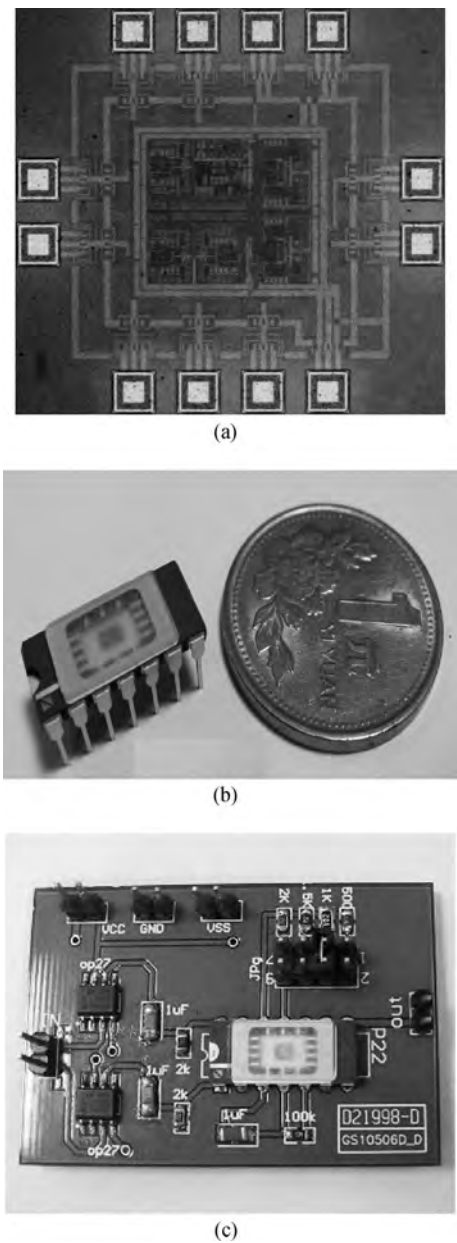


Fig. 2. Core circuit of the MENB. (a) Micrograph of the core chip of realized specific neural signal regeneration system. The area is  $0.99 \times 0.934 \text{ mm}^2$ . (b) Encapsulated chip of neural signal regeneration system. (c) MENB system.

and Use of Laboratory Animals, which comply with international rules and policies. The toads used in the present study were purchased from a local supplier (Shengming Research Animal Farms, Nanjing, China) in the weight range of 45–55 g. Before experiments, one spinal toad (whose brain was cut but spinal cord kept intact) was prepared. A longitudinal incision was made through the skin of the dorsal side of the upper leg, and the sciatic nerve was exposed by pulling apart the muscle bundles. The sciatic nerve was freed from surrounding tissue, with care taken to avoid damage to the femoral artery and vein that run alongside the nerve. The sciatic nerve was exposed between biceps femora and semi-membranous.

The MENB is a set used as a bridge between two spinal toads' left sciatic nerves by two pairs of cuff electrodes ( $d$ :

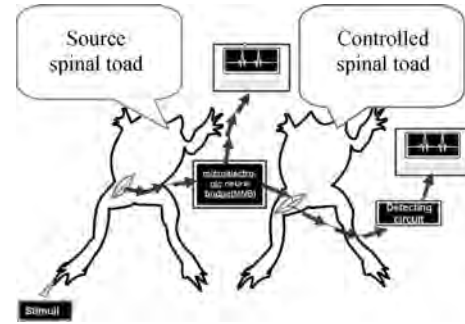


Fig. 3. Experimental strategy of the signal regeneration between the sciatic nerves of two toads, under a stimulation of 0.05 mL 5% acetic acid.

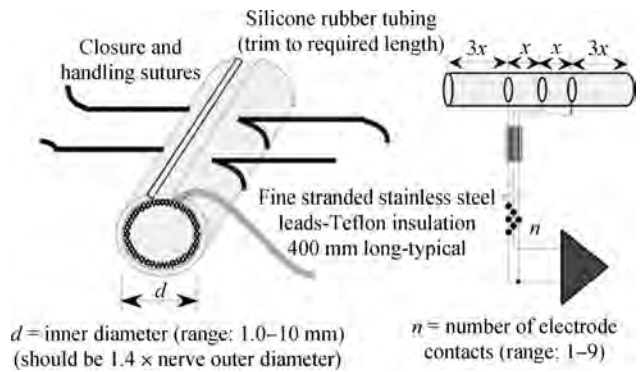


Fig. 4. Cuff electrodes of MicroProbes Company.

1.5 mm;  $x$ : 2 mm;  $n$ : 4), as shown in Fig. 4 (MicroProbes Company, USA). One pair of cuff electrodes was contacted on the left sciatic nerve of the source spinal toad, which would be stimulated by exterior chemical stimulation. The cable connector connected the input of the MENB. Another pair of electrodes contacted with the output of the MENB. Both spinal toads were actionless in the absence of external stimulation. After 0.05 mL 5% acetic acid was dropped on the toe of the source spinal toad's leg, sciatic nerve signals of both toads were monitored and recorded.

### 2.3. Data processing

In order to verify the success of the microelectronic neural bridge, we need to compare the sciatic signals of the source spinal toad and of the controlled spinal toad through correlation function analysis.

The coherence function  $\rho_{xy}$  is defined as

$$\rho_{xy}^2 = \frac{\left[ \sum_{n=-\infty}^{+\infty} x(n)y(n+m) \right]^2}{\sum_{n=-\infty}^{+\infty} x^2(n) \sum_{n=-\infty}^{+\infty} y^2(n)}$$

where  $x(n)$  and  $y(n)$  are discrete signals;  $m$  is the number of shift points and delay time;  $m > 0$  means that sequence  $y(n)$  is shifted leftwards, while  $m < 0$  means that sequence  $y(n)$  is shifted to the right. We can get different  $\rho_{xy}$  with different  $m$  values.

The coherence function is a normalized correlation function, and it can measure the relative linearity and delay time

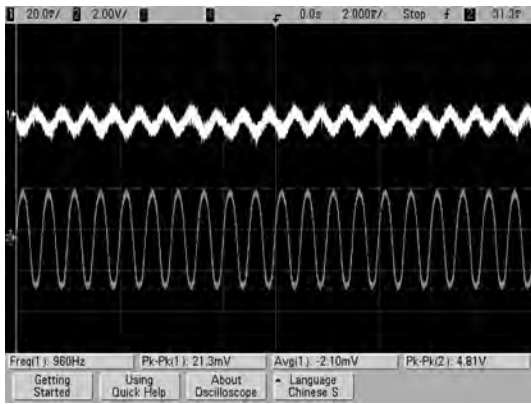


Fig. 5. Waveform graphs of MENB testing: the input signal is a sine signal with  $V_{in} = 8 \text{ mV}_{PP}$ ,  $f = 1 \text{ kHz}$ .

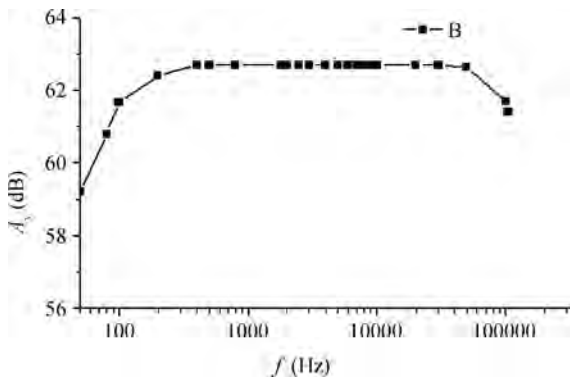


Fig. 6. Amplitude–frequency characteristic of MENB:  $R_g = 200 \Omega$ ,  $R_L = 20 \text{ k}\Omega$ .

between two signals. The coherence value has nothing to do with the magnitude of the oscillatory signals and is convenient for comparing the degree of relativity. It can express not only the phase coherence but also the phase-shift (and delayed) coherence. The coherence value indicates the strength of the coupling in the time domain. It is mathematically bounded between the negative one and the positive one, where one indicates a perfect linear relationship and zero indicates that the two signals are not coherent.

### 3. Results

#### 3.1. Test results

When we tested the electrical characteristics of a MENB, the test condition was  $R_g = 200 \Omega$ . The first channel in Fig. 5 shows the input signal, which is a sinusoidal signal with  $V_{in} = 8 \text{ mV}_{pp}$  and  $f = 1 \text{ kHz}$ . The second channel in Fig. 5 shows the output signal of the MENB. Because the waveform generator used for the test is Agilent 33220, the minimum signal amplitude is  $20 \text{ mV}_{pp}$ . Here, the input signal is attenuated to  $8 \text{ mV}_{pp}$ . Figure 6 shows the measured amplifier transfer function from  $50 \text{ Hz}$  to  $10^5 \text{ Hz}$ . The midband gain is  $62.7 \text{ dB}$ . The low-frequency cutoff is approximately  $60 \text{ Hz}$ . The amplifier’s characteristics are  $A_v = 20\lg(V_{out}/V_{in})$ ,  $R_g = 200 \Omega$ ,  $R_L = 20 \text{ k}\Omega$ . The power dissipation of the MENB is  $40 \text{ mW}$ .

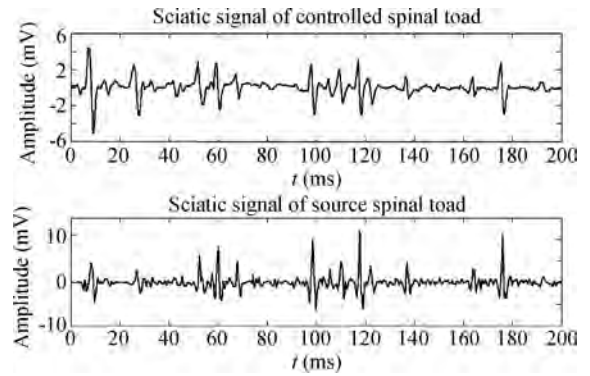


Fig. 7. Sciatic nerve signals in a regeneration experiment.

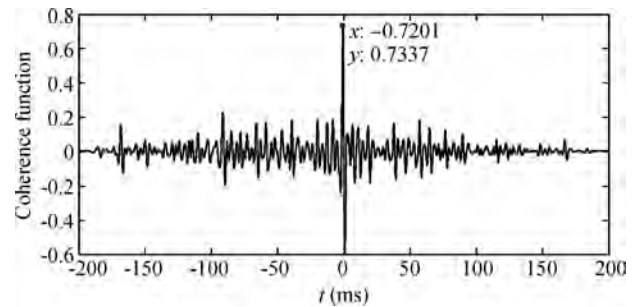


Fig. 8. Coherence function of two spinal toad’s sciatic nerve signals.

#### 3.2. Biological test results

After dropping  $0.05 \text{ mL}$   $5\%$  acetic acid on the toe of the source spinal toad’s leg, the source spinal toad flexed its left leg in a withdrawal reflex. In this case, a neural signal with a series of spikes was present in the sciatic nerve of the spinal toad. The signal, detected by the cuff electrode, is amplified and processed by the MENB. Through another cuff electrode connected with the output of the MENB, the regenerated neural signals stimulated the controlled spinal toad’s sciatic nerve. The left leg of the controlled toad made a similar action just like the source spinal toad. At the same time, sciatic nerves signals of both toads were monitored and recorded. Figure 7 shows one segment of the signal.

In order to examine the similarity between the source sciatic neural signal and regenerated sciatic neural signal on the controlled toad’s sciatic nerve, correlation analysis of the data of Fig. 7 were performed and the result is shown in Fig. 8.

The result in Fig. 8 shows that when the neural signal on the sciatic nerve of the controlled spinal toad is delayed by  $0.72 \text{ ms}$  relative to the sciatic nerve signal of the source spinal toad, the cross-correlation function reaches the maximum value of  $0.73$ .

### 4. Discussion

According to the features of neural signals and the requirements on implantable devices, typical extracellular spikes (action potentials) have amplitudes of several microvolts to  $500 \mu\text{V}$ <sup>[14]</sup>. A differential input system with a high CMRR is needed to detect the spikes because of high background noises. When we test the MENB, the first channel in Fig. 5 is the in-

put sinusoidal signal, which came from the signal generator (Agilent 33220) with an amplitude of 8 mV. Owing to the interference, the amplitude of the input signal looks higher and the wave is distorted. However, we can find that the waveform of the second channel in Fig. 5, i.e. the output of MENB, is smooth. This means that the CMRR of the MENB is high enough to detect a neural signal.

The energy of extracellular spikes (action potentials) is in the range of 100 Hz–7 kHz<sup>[14]</sup>. The 3-dB bandwidth of the amplitude-frequency characteristic of the MENB shown in Fig. 6 is 60 Hz–160 kHz, which covered the spikes' energy range completely. According to the experience obtained from earlier experiments, stimuli with amplitude equal or greater than 300–400 mV<sub>pp</sub> can inspire neural signals effectively. For the sake of integrating the detecting and the FES circuit on one chip, the gain of the MENB is defined at approximately 60 dB. The amplitude-frequency characteristic of the MENB in Fig. 6 shows that the MENB can be used not only for detecting nerve signals but also for FES. This is an important feature that is different from those recording systems or FES systems.

The interface between the electrode and the organism could have a large DC offset, which can influence the performance of the detection circuit. We can decrease this DC offset effectively by using an integral circuit including  $R_4$ ,  $C_4$ , and an operational amplifier as the feedback circuit for the three-op-amp instrumentation amplifier.

This MENB system is gradually formed and improved after lots of trial. Some of the components, such as the follower and the integral circuit, are on the PCB and haven't been integrated. Thus, the power dissipation isn't low enough yet. We are pushing our work forward on improving the integration and lower power dissipation. We hope that the whole MENB can be integrated on an implantable chip in the future.

## 5. Conclusions

A new version of the MENB that is implemented on a PCB has been developed. The MENB has been used in animal experiments. In order to avoid the conduction of the organism itself, or introduction of other interference, a special nerve regeneration experiment method has been used on sciatic nerves of different spinal toads. The result of correlation function analysis show that the regenerated signal is correlated with the source signal significantly<sup>[22]</sup>, and the MENB works well and can be used in nerve signal regeneration.

## References

- [1] Barbeau H, McCrea D A, O'Donovan M J, et al. Tapping into spinal circuits to restore motor function. *Brain Research Reviews*, 1999, 30(1): 27
- [2] Patil P G, Turner D A. The development of brain-machine interface neuroprosthetic devices. *Neurotherapeutics*, 2008, 5(1): 137
- [3] Donoghue J P. Bridging the brain to the world: a perspective on neural interface systems. *Neuron*, 2008, 60(3): 511
- [4] Shepherd R K, Coco A, Epp S B. Neurotrophins and electrical stimulation for protection and repair of spiral ganglion neurons following sensorineural hearing loss. *Hearing Research*, 2008, 242(1/2): 100
- [5] Zhang J, Zhang X. Electrical stimulation of the dorsal cochlear nucleus induces hearing in rats. *Brain Research*, 2010, 1311: 37
- [6] Wang K, Li X X, Jiang Y R, et al. Influential factors of thresholds for electrically evoked potentials elicited by intraorbital electrical stimulation of the optic nerve in rabbit eyes. *Vision Research*, 2007, 47(23): 3012
- [7] Stett A, Barth W, Weiss S, et al. Electrical multisite stimulation of the isolated chicken retina. *Vision Research*, 2000, 40(13): 1785
- [8] Fedorov A B, Chibisova A N, Tchibissova J M. Impulse modulating therapeutic electrical stimulation (IMTES) increases visual field size in patients with optic nerve lesions. *International Congress Series*, 2005, 1282: 525
- [9] Tanriverdi T, Al-Jehani H, Poulin N, et al. Functional results of electrical cortical stimulation of the lower sensory strip. *Journal of Clinical Neuroscience*, 2009, 16(9): 1188
- [10] Ajoudani A, Erfanian A, Neuro A. Sliding-mode control with adaptive modeling of uncertainty for control of movement in paralyzed limbs using functional electrical stimulation. *IEEE Trans Biomed Eng*, 2009, 56(7): 1771
- [11] Wang Z G, Lu X, Li W, et al. Study of micro-electronics for detecting and stimulating of central neural signals. *Proceedings First International Conference on Neural Interface and Control*, 2005: 192
- [12] Wang Z G, Gu X S, Lu X Y. The method and equipment for neural channel bridge aided by a micro-electronic system. *Chinese Patent*, No. 200510135541.6. December 24, 2008
- [13] Wang Z, Gu X, Lu X, et al. Microelectronics-embedded channel bridging and signal regeneration of injured spinal cords. *Progress in Natural Science*, 2009, 19(10): 1261
- [14] Harrison R R, Charles C. A low-power low-noise CMOS amplifier for neural recording applications. *IEEE J Solid-State Circuits*, 2003, 38(6): 958
- [15] Xie Shushan, Wang Zhigong, Lü Xiaoying, et al. A four-channel microelectronic system for neural signal regeneration. *Journal of Semiconductors*, 2009, 30(12): 125005
- [16] Wise K D, Sodagar A M, Yao Y, et al. Microelectrodes, microelectronics, and implantable neural Microsystems. *Proc IEEE*, 2008, 96(7): 1184
- [17] Zhao H T, Lü X Y, Wang Y F, et al. Percutaneous electromagnetic coupling. *Journal of Southeast University (Natural Science Edition)*, 2007, 37(2): 368
- [18] Nielsen J H, Lehmann T. An implantable CMOS amplifier for nerve signals. *The 8th IEEE International Conference on Electronics, Circuits and Systems, ICECS*, 2001, 3: 1183
- [19] Wang Yufeng, Wang Zhigong. A single-chip and low-power CMOS amplifier for neural signal detection. *Chinese Journal of Semiconductors*, 2006, 27(8): 1490
- [20] Li W Y, Wang Z G. Integrated circuit for single channel neural signal regeneration. *Journal of Southeast University (English Edition)*, 2008, 24(2): 155
- [21] Xie Shushan, Wang Zhigong, Lü Xiaoying, et al. A four-channel microelectronic system for neural signal regeneration. *Journal of Semiconductors*, 2009, 30(12): 125005
- [22] <http://wenku.baidu.com/view/ba40b22d7375a417866f8f73.html>